


High-grade serous carcinomas arise in the mouse oviduct via defects linked to the human disease

Yali Zhail, Rong Wu¹, Rork Kuick², Michael S Sessine¹, Stephanie Schulman¹, Megan Green¹, Eric R Fearon^{1,3,4} and Kathleen R Cho^{1,3,*} 

¹ Department of Pathology, University of Michigan Medical School, Ann Arbor, MI, USA

² Department of Biostatistics, University of Michigan School of Public Health, Ann Arbor, MI, USA

³ Department of Internal Medicine, University of Michigan Medical School, Ann Arbor, MI, USA

⁴ Department of Human Genetics, University of Michigan Medical School, Ann Arbor, MI, USA

*Correspondence to: KR Cho, 1506 BSRB, 109 Zina Pitcher Place, University of Michigan, Ann Arbor, MI 48109-2200, USA. E-mail: kathcho@umich.edu

Abstract

Recent studies have suggested that the most common and lethal type of 'ovarian' cancer, i.e. high-grade serous carcinoma (HGSC), usually arises from epithelium on the fallopian tube fimbriae, and not from the ovarian surface epithelium. We have developed *Ovgp1-iCreER^{T2}* mice in which the *Ovgp1* promoter controls expression of tamoxifen-regulated Cre recombinase in oviductal epithelium – the murine equivalent of human fallopian tube epithelium (FTE). We employed *Ovgp1-iCreER^{T2}* mice to show that FTE-specific inactivation of several different combinations of tumour suppressor genes that are recurrently mutated in human HGSCs – namely *Brca1*, *Trp53*, *Rb1*, and *Nf1* – results in serous tubal intraepithelial carcinomas (STICs) that progress to HGSC or carcinosarcoma, and to widespread metastatic disease in a subset of mice. The cancer phenotype is highly penetrant and more rapid in mice carrying engineered alleles of all four tumour suppressor genes. *Brca1*, *Trp53* and *Pten* inactivation in the oviduct also results in STICs and HGSCs, and is associated with diffuse epithelial hyperplasia and mucinous metaplasia, which are not observed in mice with intact *Pten*. Oviductal tumours arise earlier in these mice than in those with *Brca1*, *Trp53*, *Rb1* and *Nf1* inactivation. Tumour initiation and/or progression in mice lacking conditional *Pten* alleles probably require the acquisition of additional defects, a notion supported by our identification of loss of the wild-type *Rb1* allele in the tumours of mice carrying only one floxed *Rb1* allele. Collectively, the models closely recapitulate the heterogeneity and histological, genetic and biological features of human HGSC. These models should prove useful for studying the pathobiology and genetics of HGSC *in vivo*, and for testing new approaches for prevention, early detection, and treatment.

Copyright © 2017 Pathological Society of Great Britain and Ireland. Published by John Wiley & Sons, Ltd.

Keywords: ovarian cancer; genetically engineered mouse model; fallopian tube; serous carcinoma

Received 10 March 2017; Revised 9 May 2017; Accepted 24 May 2017

No conflicts of interest were declared.

Introduction

High-grade serous carcinoma (HGSC) is the most common and lethal type of 'ovarian' cancer, accounting for ~70–75% of cases [1]. Recent studies have suggested that HGSCs usually arise in the fallopian tube epithelium (FTE), rather than in the ovarian surface epithelium (OSE) [2,3]. HGSCs show a high level of chromosomal instability, and almost all of them harbour somatic *TP53* mutations, which occur very early in HGSC pathogenesis, as *TP53* mutations are also present in HGSC precursors, known as serous tubal intraepithelial carcinomas (STICs) [4–6]. Although only nine genes were shown to be significantly mutated in HGSCs by the Cancer Genome Atlas project [7], somatic structural alterations (e.g. DNA copy number alterations, gene breakage, and gene fusions) are frequently seen in these tumours [7,8]. These mutational

and structural changes often lead to dysfunction of the RB, BRCA, phosphoinositide 3-kinase (PI3K) and RAS pathways. Genetic instability in the early lesions presumably contributes to the likelihood that somatic mutations conferring metastatic potential will be acquired. Thus, women with HGSCs typically have small primary lesions and widespread metastases at diagnosis. Ovarian carcinosarcomas [also known as malignant mixed Müllerian tumours (MMMTs)] show both malignant epithelial and mesenchymal elements, and are now thought to represent a much less common variant of HGSC [9]. Like HGSCs, pelvic/ovarian carcinosarcomas have been associated with STICs, and a recent study showed identical *TP53* mutations in matched pairs of STICs and carcinosarcomas, providing evidence for their clonal relationship and the potential origin of carcinosarcoma in the fallopian tube [10,11].

Genetically engineered mouse models (GEMMs) of ovarian cancer that closely recapitulate their human tumour counterparts provide excellent *in vivo* systems with which to study tumour biology, and to perform preclinical studies aimed at improving ovarian cancer prevention, early detection, and therapy [12]. Historically, most HGSC GEMMs were based on OSE transformation [13–16]. More recently, models based on transformation of oviduct (equivalent to human fallopian tube) epithelium (hereafter referred to as FTE) have been reported. Kim *et al.* developed an oviductal HGSC model based on conditional deletion of *Dicer* and *Pten*, using the *Amhr2* promoter to express Cre recombinase in the murine oviduct [17]. The tumours in this model arise first in the fallopian tube stroma and are initially mesenchymal. More recently, Perets *et al.* described an HGSC GEMM, using the *Pax8* promoter to drive Cre-mediated recombination of floxed *Brca1* or *Brca2*, *Pten* and *Trp53* alleles in the FTE of *Pax8-rtTA;TetO-Cre* mice [18]. Although these oviductal HGSC models represent a significant advance, both direct Cre expression by using gene promoters that lack specificity for the FTE. *Amhr2* is also expressed in the OSE and stromal cells in the ovary, oviduct, and other portions of the female genital tract [19], whereas *Pax8* is expressed in other Müllerian epithelia, such as endometrial glandular epithelium, as well as other sites such as the kidney and thyroid [20]. A promoter for directing Cre expression to the FTE with greater specificity was highlighted by Miyoshi *et al.*, who reported the development of oviductal HGSC-like tumours in mice expressing SV40-LTag under control of a 2.2-kb fragment of the murine *Ovgp1* (oviductal glycoprotein 1) promoter [21]. We have developed mice in which the *Ovgp1* promoter directs expression of tamoxifen (TAM)-regulated Cre recombinase in the FTE [22]. *Ovgp1-iCreER^{T2}* mice carrying floxed alleles of the *Apc* and *Pten* tumour suppressor genes (TSGs) invariably develop endometrioid-like tumours in the FTE following treatment with TAM, and these tumours are more similar to human ovarian endometrioid carcinomas in their morphology, biological behaviour and gene expression profiles than tumours based on *Apc* and *Pten* inactivation in the OSE [22]. Whereas our earlier work showed that the cell of origin has a profound impact on the tumour phenotype, in the present study we wished to test the hypothesis that genetics also affect the tumour phenotype. Given that dysregulation of Wnt and PI3K–AKT signalling – which is characteristic of human endometrioid carcinomas – in the oviductal epithelium results in mouse tumours with endometrioid-like morphology, we wanted to test whether inactivation of TSGs that are often mutated in human HGSCs (*Brca1*, *Trp53*, *Rb1*, and *Nf1*) [7] leads to HGSC-like tumours in the mouse oviduct. To build on the work of Perets *et al.*, we also wished to test the effects of *Brca1*, *Trp53* and *Pten* inactivation in our model system [18]. Although somatic *PTEN* point mutations are relatively uncommon in HGSCs, dysregulation of the PI3K–AKT signalling pathway is frequently observed, often as a consequence

of *PTEN* gene breakage events or *PIK3CA* amplification [7,8].

Materials and methods

Genetically modified mice and animal care

The development and characterization of *Ovgp1-iCreER^{T2}* transgenic mice have been described in detail [22]. *Ovgp1-iCreER^{T2}* transgenic mice were crossed with mice carrying engineered *Rb1*, *Trp53*, *Brca1*, *Nf1* and *Pten* alleles, to generate transgenic mice with various combinations of TSG alterations. In addition to floxed *Rb1*, *Trp53*, *Brca1*, *Nf1* and *Pten* alleles in which Cre-mediated recombination generates null alleles, we employed mice carrying a Cre-inducible *Trp53* mutation (LSL-R172H) and mice with constitutional inactivation of one *Brca1* allele (*Brca1^{del}*). *Rb1^{fl}*, *Trp53^{fl}*, *Trp53^{LSL-R172H}* and *Brca1^{fl}* mice were obtained from the National Cancer Institute's mouse repository. *Nf1^{fl/fl}* mice were a gift from Yuan Zhu (currently at the Children's National Medical Center, Washington, DC, USA). *Pten^{fl/fl}* mice were a gift from Tak Mak (University Health Network, Toronto, Ontario, Canada). Mice with the *Brca1^{del}* allele were generated by crossing *E2a-Cre* mice (B6.FVB-Tg[EIIa-cre]C5379Lmgd/J; Jackson Laboratory, Bar Harbor, ME, USA) with *Brca1^{fl/+}* mice to generate mice carrying an inactivated *Brca1* allele in the germline. All strains were maintained on a mixed genetic background. Mouse genotypes were confirmed by polymerase chain reaction (PCR) analysis of tail DNA (primer sequences are shown in supplementary material, Table S1). Procedures involving mice were approved by the University of Michigan's Institutional Animal Care and Use Committee (PRO00006370).

In vivo induction of oviductal tumours

Ovgp1-iCre-ER^{T2} female mice carrying various engineered TSG alleles were given intraperitoneal injections of TAM (T5648; Sigma-Aldrich, Indianapolis, IN, USA) at 100 mg/kg body weight on three consecutive days, usually when mice were aged 6–8 weeks. Initially, while mice were monitored for tumour development, selected mice were killed at various time points following TAM injection and inspected for tumour location and extent at necropsy. Thirteen mice underwent survival surgery, during which the right oviduct and ovary were removed at 2 months ($n = 11$), 3 months ($n = 1$) or 12 months ($n = 1$) after TAM injection, and the mice were then monitored for tumour development in the remaining oviduct. Once the presence of a tumour had been established, most mice were monitored to humane endpoints. Mice were grossly evaluated for tumour extent, and, in each case, ovaries, oviducts, uteri, lungs, multiple abdominal organs, omentum and mesentery were examined microscopically.

Histopathology and immunohistochemistry

Tissues were fixed in 10% buffered formalin and paraffin-embedded. Sections (5 µm) were haematoxylin and eosin (H&E)-stained for evaluation by light microscopy. To identify microscopic oviductal lesions, each oviduct and ovary were serially sectioned in their entirety for microscopic examination. Alternate sections were either stained with H&E or retained for immunohistochemical (IHC) staining, performed according to standard methods as previously described [22]. Antigen retrieval was performed by microwaving the slides in citrate buffer, pH 6.0 (Biogenex, San Ramon, CA, USA) for 15 min. Antigen-antibody complexes were detected with the avidin-biotin peroxidase method, with diaminobenzidine as the chromogenic substrate (Vectastain ABC kit; Vector Laboratories, Burlingame, CA, USA). The primary antibodies used were: rat anti-cytokeratin (CK) 8 (Developmental Studies Hybridoma Bank, University of Iowa), rabbit anti-p53 and rabbit anti-PAX8 (Proteintech, Chicago, IL, USA), rat anti-Ki67 (Dako, Carpinteria, CA, USA), and goat anti-OVGPI (Santa Cruz Biotechnology, Santa Cruz, CA, USA).

Results

STICs, HGSCs and MMMTs develop in the mouse oviduct following conditional inactivation of various combinations of *Rb1*, *Brcal*, *Trp53* and/or *Nf1* in the FTE

We crossed *Ovgp1-iCreER^{T2}* mice with mice carrying *Brcal*, *Trp53*, *Rb1* and *Nf1* alleles, to generate 80 transgenic mice of several different genotypes (Figure 1; supplementary material, Table S2). Mice with conditionally modified *Brcal*, *Trp53* and *Rb1* alleles are hereafter referred to collectively as *BPR* mice (*n* = 29). *BPN* mice (*n* = 3) are those with modified *Brcal*, *Trp53* and *Nf1* alleles, whereas *BPRN* mice (*n* = 48) carry modified alleles for all four TSGs. Data summarizing the oviductal lesions developing in these mice are shown in Figure 1, in which mice with generally similar genotypes are grouped together.

In order to determine whether *Brcal*, *Trp53*, *Rb1* and/or *Nf1* inactivation in the FTE results in an oviductal tumour phenotype, 10 mice with a range of defined genotypes were killed 1.5–6.5 months after TAM injection. One *BPRN* mouse (no. 2820) showed a microscopic lesion closely resembling human STIC in one oviduct 2.5 months after TAM injection. Oviductal lesions were not identified in the remaining nine mice. In an attempt to reduce the number of mice needed to determine whether, and how often, mice with different genotypes acquire oviductal tumours, the right oviduct and ovary were removed from 13 mice in a survival surgery procedure. Eleven of the 13 (four *BPRN*, six

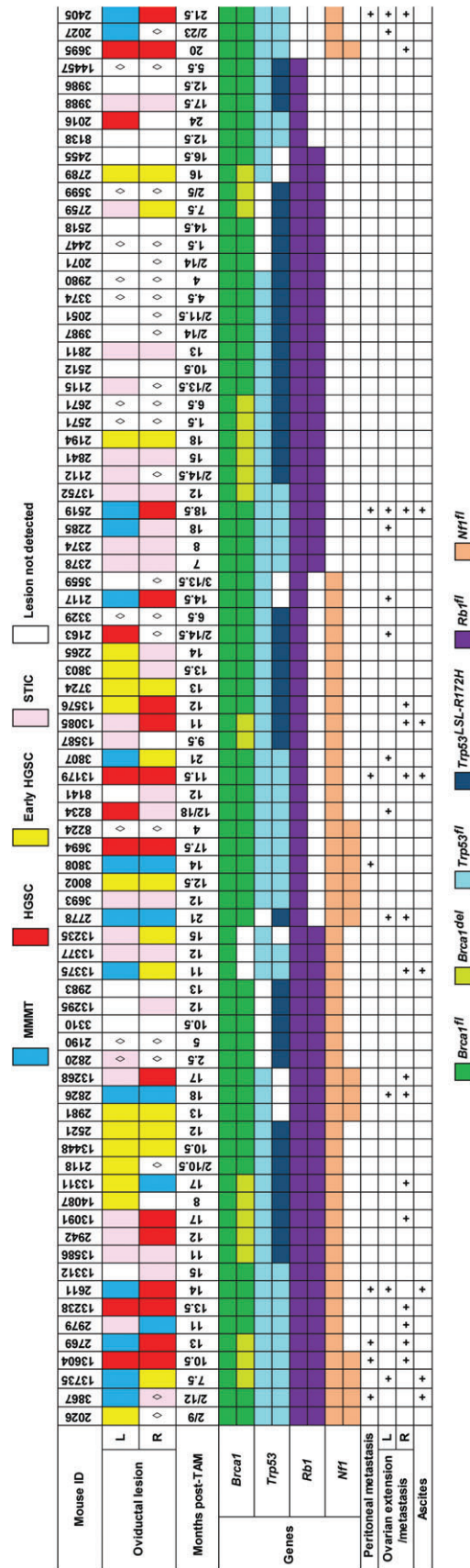


Figure 1. Summary of oviductal tumour phenotype in TAM-treated *Ovgp1-iCreER^{T2}* mice carrying various engineered *Brcal*, *Rb1*, *Trp53* and *Nf1* alleles. Data from all 80 mice are shown. Months post-TAM indicates the time points at which mice were killed. Where two time points are shown, the first represents months post-TAM at the time of survival surgery (removal of right ovary and oviduct) and the second represents months post-TAM at the time of death. The diamond symbol marks oviducts evaluated ≤6.5 months post-TAM.

BPR, and one *BPN*) had the right oviduct and ovary removed 2 months after TAM injection. STIC was found in one *BPRN* mouse (no. 3867, with homozygous floxed alleles for all four TSGs). Two additional *BPRN* mice underwent survival surgery at 3 and 12 months after TAM injection (no. 3559 and no. 8234), and STIC was identified in the latter. Photomicrographs of two representative mouse STIC lesions are shown in Figure 2. Like STICs in humans, mouse STICs have a predilection for arising in the distal portion of the oviduct (Figure 2A, C, equivalent to human fallopian tube fimbriae). The lesional cells show enlarged, hyperchromatic and pleomorphic nuclei, prominent nucleoli, increased mitotic activity, and loss of polarization (Figure 2B, D).

All 13 mice that underwent survival surgery were monitored for tumour development in the remaining oviduct for 5–23 months following TAM injection. Lesions were identified in the remaining oviduct in five of six *BPRN* mice, in two of six *BPR* mice, and in the *BPN* mouse. The oviductal lesions identified in the remaining oviduct included two STICs, two early HGSCs (confined to the oviduct), two HGSCs extending beyond the oviduct, and two MMTs, one of which metastasized widely.

Oviductal lesions (STIC, early HGSC, HGSC, and/or MMT) were identified in 50 of 57 additional mice (12 *BPR*, 36 *BPRN* and two *BPN* mice) not included in the groups described above. These mice were monitored for tumour development for time periods ranging from 7 to 24 months after TAM injection (Figure 1). In the 59 of 80 mice with oviductal lesions, tumour involved one or both ovaries in 24 (41%), obliterating the ovary in all but four cases. Widespread peritoneal metastases were observed in eight mice (14%) and ascites in seven mice (12%). In similar fashion to the human disease, metastases were often observed in the omentum. Representative photomicrographs showing tumour progression from STIC to early HGSC, HGSC/MMMT and metastatic disease are shown in Figure 3, and IHC staining of primary tumours at various stages of tumour progression, and metastases to omentum and ovary, are shown in Figure 4 and supplementary material, Figure S1, respectively. The tumour cells expressed CK8 and PAX8, and showed increased proliferation, based on IHC staining for Ki67. Tumours with the conditional *Trp53* R172H mutant allele only occasionally showed focal stabilization of p53 (Figure 4; no. 3724). Whereas the neoplastic cells in STICs and HGSCs retain expression of PAX8, a marker of secretory cells, they do not express tubulin, which marks ciliated cells (supplementary material, Figure S2). The absence of tubulin expression is not surprising, as human HGSCs and STICs do not typically show ciliated morphology.

Only six of 48 (12.5%) *BPRN* mice, as compared with 15 of 29 (52%) *BPR* mice, failed to develop lesions. Some of the failures were probably attributable to mice being killed at relatively early time points (≤ 6.5 months after TAM injection), particularly in the *BPR* mice. All

three *BPN* mice included in the study developed oviductal HGSC and/or MMT. On a per oviduct basis, and excluding those removed at the time of survival surgery or evaluated earlier than 7 months after TAM injection, 87 oviducts had at least one floxed *Nfl* allele. In these oviducts, 11% had no neoplastic lesions, 21% had STIC, 25% had early HGSC, and 43% had HGSC/MMMT. In contrast, for the 39 oviducts without floxed *Nfl*, the percentages were 36%, 41%, 13%, and 10%, respectively ($P = 3.8 \times 10^{-5}$, chi-squared test; $P = 2.7 \times 10^{-6}$, Mantel–Haenszel chi-squared test of association). On the basis of our analysis of the data shown in Figure 1 and in supplementary material, Table S2, we conclude that the HGSC phenotype in our model is highly penetrant in *BPRN* and *BPN* mice, especially those carrying homozygous floxed alleles for all TSGs. Furthermore, disease progression is generally more rapid in *BPRN* than in *BPR* or *BPN* mice.

Cre-mediated recombination of *Brcal*, *Trp53*, *Rb1* and *Nfl* alleles in representative tumours was confirmed by PCR (supplementary material, Figure S3). Interestingly, in mice carrying one floxed and one wild-type *Rb1* allele, loss of the wild-type *Rb1* allele was seen in seven of eight tumours analysed (e.g. supplementary material, Figure S3, nos. 13085, 13576, 13179, and 2117). Hence, as in human HGSC pathogenesis, the mouse tumours acquire additional genetic alterations during tumour progression. We evaluated oviductal tumour DNA for activation of the conditional *Trp53*^{LSL-R172H} mutant allele in three representative tumours, two of which are shown in supplementary material, Figure S3C. In all three tumours, recombination of the conditional mutant *Trp53* allele was not observed. Interestingly, of mice with both oviducts intact for ≥ 7 months, three of six with the *Trp53*^{LSL-R172H/+} genotype had no detectable oviductal lesions, whereas only four of 51 mice with at least one floxed *Trp53* allele lacked lesions ($P = 0.020$, two-sided Fisher's exact test). These findings suggest that in this HGSC model system: (1) there is selection for biallelic inactivation of *Rb1*; and (2) the *Trp53*^{fl} allele, generating a null *Trp53* mutation via Cre recombination, is preferable to the *Trp53*^{LSL-R172H} mutant allele, perhaps because of inefficient Cre recombination or the absence of selective pressure for recombination and/or selection against recombination. It is of note that, in the absence of Cre-mediated activation of the R172H mutation, the *Trp53*^{LSL-R172H} allele is null [23].

In addition to the oviductal tumours, non-Müllerian tumours (e.g. lymphomas, soft tissue sarcomas, and adenomas/carcinomas of the thyroid, lung, skin, or breast) were identified in a subset of mice. Lymphomas were the most common non-oviductal tumours (17/80; 21%). Interestingly, three of five mammary carcinomas arose in mice carrying one constitutional inactivated *Brcal* allele. The development of lymphomas, sarcomas, carcinomas and other tumour types has been reported in various mouse strains, including some with high incidence rates [24–26]. Hence, the development of non-oviductal tumours is not unexpected,

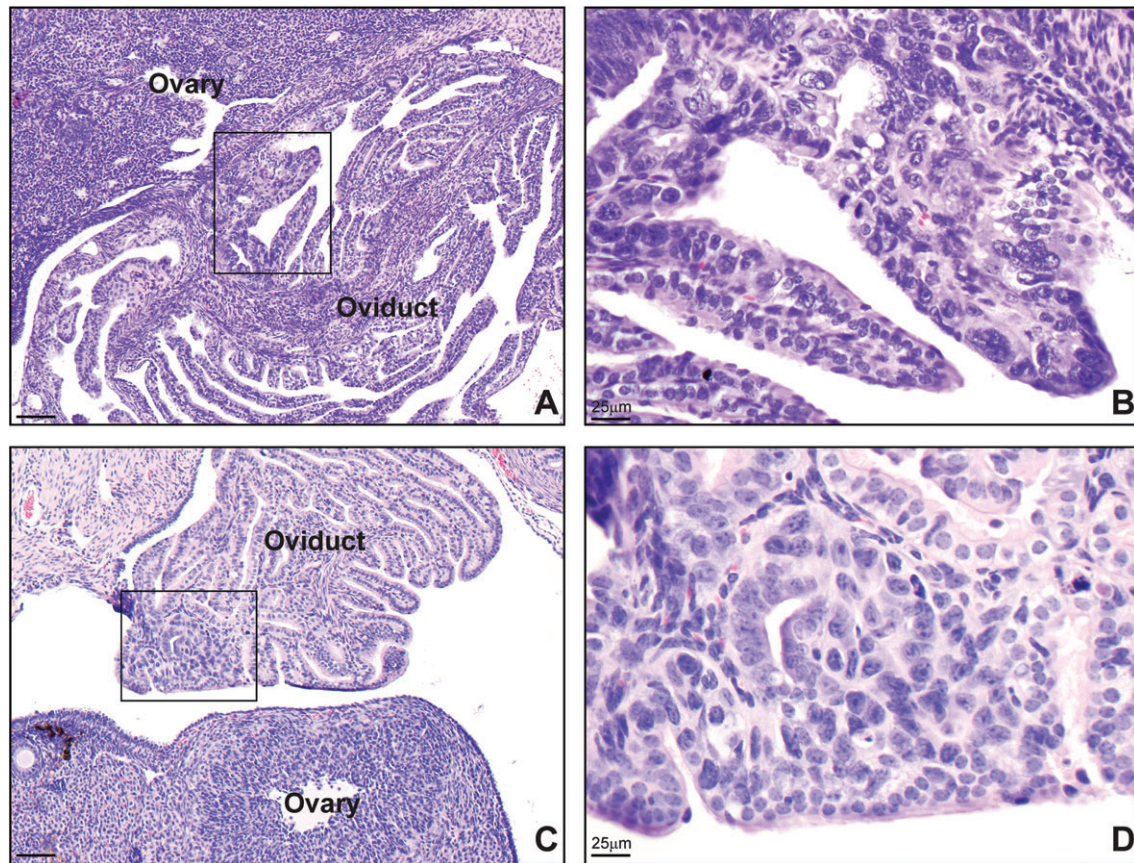


Figure 2. Representative photomicrographs of STICs arising in *BPRN* mice. (A) Oviduct from mouse no. 8141, showing STIC (boxed region) arising in a portion of the oviduct in close proximity to the ovary. (B) Higher magnification of the boxed region in (A). (C) Oviduct from mouse no. 8234, showing STIC (boxed region) in the distal oviduct. (D) Higher magnification of the boxed region in (C). Scale bars: 100 μm unless otherwise indicated.

given the advanced age of many of the mice and the presence of mutant *Brcal* and/or *Trp53* alleles in the germline of a sizeable subset. In order to determine whether Cre-mediated recombination occurred in the non-Müllerian tumour cells, we evaluated DNA from representative tumours for the presence of recombined *Brcal*, *Trp53*, *Rbl* and *Nfl* alleles (supplementary material, Figure S4). We found Cre-mediated recombination of engineered TSG alleles in one endometrial carcinoma (not shown) and in the presumptive thyroid carcinomas, which had morphological features reminiscent of human medullary carcinoma. The remaining tumours appear to have arisen spontaneously. We did not observe OVGP1 expression in the thyroid based on IHC staining, and hence allelic recombination in this site appears to be independent of endogenous *Ovgp1* expression.

TAM-treated *Ovgp1-iCreER^{T2};Brcal^{fl/fl};Trp53^{fl/fl};Pten^{fl/fl}* (*BPP*) mice develop STICs, HGSCs, and MMMTs, and also show oviductal epithelial hyperplasia and mucinous metaplasia

We crossed *Ovgp1-iCreER^{T2}* mice with mice carrying floxed *Brcal*, *Trp53* and *Pten* alleles, to generate *Ovgp1-iCreER^{T2};Brcal^{fl/fl};Trp53^{fl/fl};Pten^{fl/fl}* (*BPP*) mice. Ten mice were treated with TAM, and two were killed

at each of five time points (1, 2, 3, 4 and 6 months after TAM injection). STICs or early HGSC-like lesions were already present in treated mice 1 month after TAM injection. All 10 mice developed bilateral oviductal lesions, including oviductal carcinomas at the later time points. One *BPP* mouse, examined 6 months after TAM injection, developed carcinosarcoma with metastasis to the ovary and ascites. Endometrial hyperplasia near the junction of the uterine horn with the oviduct was noted in two of the 10 *BPP* mice. Data from the *BPP* mice are summarized in supplementary material, Table S3, and representative photomicrographs of H&E-stained and immunostained lesions arising in the oviducts of *BPP* mice at 1, 2 and 6 months after TAM injection are shown in Figure 5. Like tumours arising in *BPR*, *BPRN* and *BPN* mice, oviductal STICs (Figure 5A, B), HGSCs (Figure 5E, F, I, J) and MMMTs (Figure 5M, N) arising in *BPP* mice expressed CK8 (Figure 5C, G, K, O) and PAX8 (Figure 5D, H, L, P). As expected, they lacked expression of PTEN, and had an increased Ki67 proliferative index (not shown). In addition, the oviducts of the TAM-treated *BPP* mice showed rather diffuse epithelial hyperplasia characterized by areas with increased epithelial stratification, as well as mucinous metaplasia (Figure 6) in which the cells showed prominent cytoplasmic

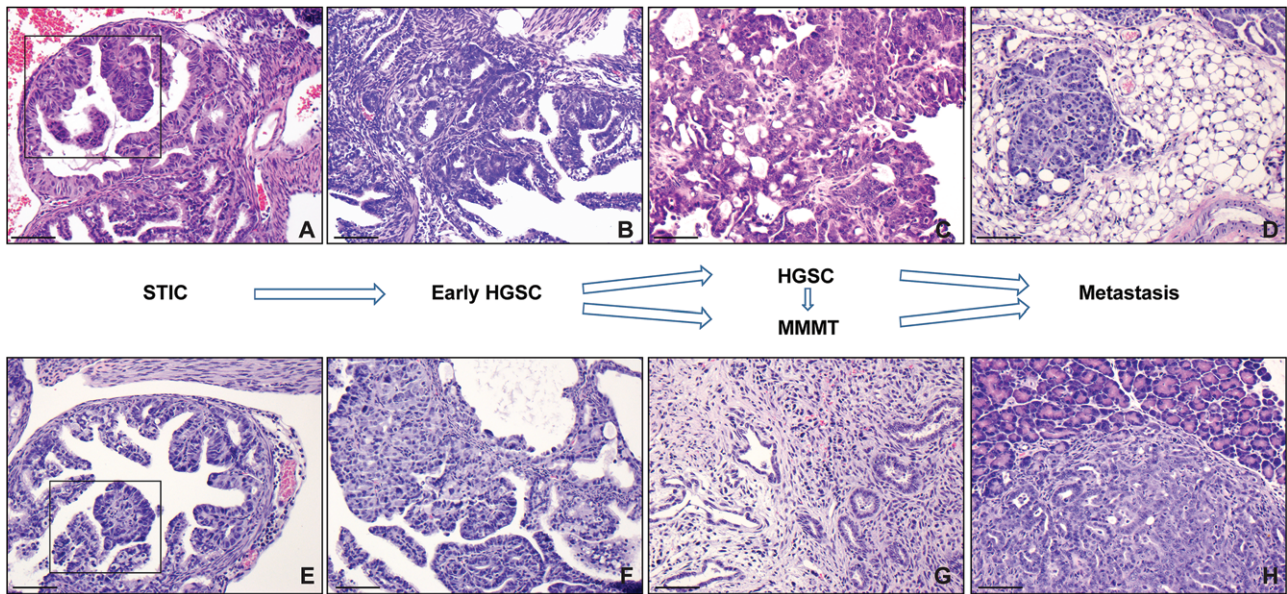


Figure 3. Representative photomicrographs of H&E-stained sections showing progression of oviductal lesions in *BPRN* mice. STICs (A and E), early HGSCs (B and F), HGSC (C), MMTT (G) and metastases to omentum (D) and pancreas (H) are shown. Scale bars: 100 μ m.

accumulation of both acidic (Alcian Blue-positive) and neutral (periodic acid–Schiff-positive) mucin as compared with normal oviductal epithelium. These latter findings were not seen in *BPR*, *BPN* or *BPRN* mice. None of the *BPP* mice developed non-oviductal malignancies during the 6-month surveillance period.

Discussion

GEMMs that closely mimic the origin, genetics and biological behaviour of HGSC would potentially be of great utility for testing strategies to improve HGSC prevention, early diagnosis, and treatment. Here, we have shown that *Ovgp1-iCreER^{T2}* mice carrying conditional mutant TSG alleles relevant to human HGSC pathogenesis develop oviductal STICs, HGSCs and carcinomas that frequently metastasize to the ovaries and/or peritoneum and other organs. Although this is not the first GEMM to target the clinically relevant FTE, it does so with greater specificity than previously described models employing the *Pax8* or *Amhr2* promoter to direct expression of Cre recombinase in the oviductal epithelium.

We have previously shown that biallelic inactivation of *Apc* and *Pten* leads to very different tumour phenotypes when induced in the OSE versus the FTE, with the oviductal tumours closely resembling human endometrioid carcinomas, and the ovarian tumours being more poorly differentiated [22]. In other words, cell of origin plays an important role in determining tumour phenotype. We now show that different combinations of genetic alterations in the FTE also lead to very different tumour phenotypes. In short, whereas genetic alterations (e.g. *Apc* and *Pten* inactivation) that dysregulate signalling pathways characteristic of human

endometrioid carcinomas result in endometrioid-like tumours in the mouse FTE [22], mutations commonly seen in human HGSCs result in HGSC-like oviductal tumours. Furthermore, although *BPR*, *BPRN*, *BPN* and *BPP* mice all develop oviductal STICs and HGSCs/MMMTs following treatment with TAM, the timing of tumour development and progression varies significantly among the different models, and the lesions are not morphologically identical. Specifically, tumour development is very rapid and penetrant in *BPP* mice, and the FTE acquires diffuse changes (hyperplasia and mucinous metaplasia) not observed in *BPR*, *BPN* or *BPRN* mice. The short latency and rapid disease progression in *BPP* mice bear some similarity to our prior findings that mice rapidly develop oviductal endometrioid-like carcinomas following biallelic *Apc* and *Pten* inactivation by the *Ovgp1-iCreER^{T2}* transgene [22]. In *BPP* and *Apc^{fl/fl};Pten^{fl/fl}* mice, the rapidity of tumour development suggests that the conditional alterations are sufficient for neoplastic transformation of the targeted cells. In contrast, in *BPR*, *BPN* and *BPRN* mice, even those with homozygous floxed alleles for all TSGs, oviductal tumours take longer to develop and progress. Progression from STIC to HGSC/MMMT usually takes well over a year in *BPR* mice, but is accelerated by addition of biallelic *Nf1* inactivation. These findings suggest that tumour initiation and/or progression in *BPR*, *BPN* and *BPRN* mice probably require the acquisition of additional defects, a notion supported by our identification of loss of the wild-type *Rb1* alleles in the tumours of mice carrying only one floxed *Rb1* allele. The relatively long latency and presumptive need for additional genetic alterations may actually be considered advantageous features of the model system, as the resultant tumour heterogeneity may more closely mimic HGSC pathogenesis in humans than the rapid

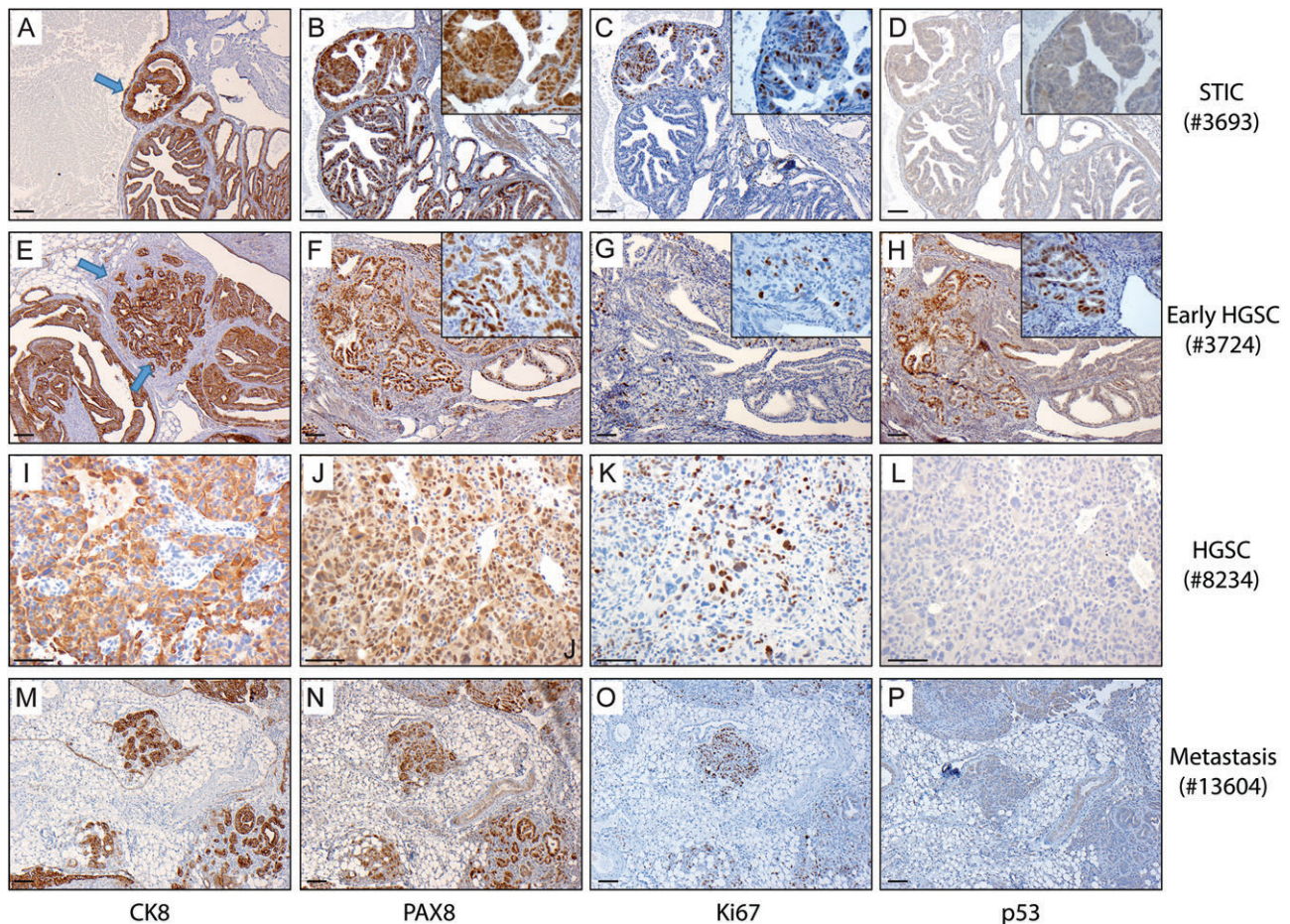


Figure 4. STICs and HGSCs arising in *BPRN* mice express markers characteristic of human HGSCs. IHC staining for CK8, PAX8, Ki67 and p53 in representative STIC (A–D), early HGSC (E–H), HGSC (I–L) and metastatic HGSC (M–P) is shown. Like normal oviductal epithelium, the tumour cells express CK8 and PAX8 – areas of CK8-expressing STIC and early HGSC are marked with blue arrows. The neoplastic cells have a high proliferative index, based on expression of Ki67. Overexpression of p53 is observed in occasional tumours with the *Trp53*^{LSL-R172H} allele (mouse no. 3724), but not in mice carrying only *Trp53*^{fl} alleles (no. 3693, no. 8234, and no. 13604). Insets in selected panels show lesional epithelium at higher magnification.

neoplastic transformation of the FTE observed in the context of *Apc/Pten* or *Brcal/Trp53/Pten* inactivation. Further analyses (e.g. whole-exome sequencing and comprehensive gene expression profiling) of the oviductal mouse HGSCs/MMMTs and comparison with human HGSCs will be needed to specifically address this issue.

A potential shortcoming of our model system is the development of non-oviductal tumours in a sizeable proportion of the 80 mice included in the study. This is probably related, at least in part, to the relatively long latency and time required for tumour progression, particularly in *BPR* and *BPN* mice. Our data suggest that this problem can be mitigated by focusing future work on TAM-treated *BPP* or *BPRN* mice with homozygous floxed alleles (or, in the case of *Brcal*, *Brcal*^{fl/del} alleles), which usually acquire STICs, HGSCs/MMMTs and metastatic disease before they develop non-oviductal tumours that necessitate early euthanasia.

Although the specific cell of origin of HGSC in humans remains unclear, our findings indicate that a population of *Ovgpl*-expressing cells in the oviduct is susceptible to transformation by somatic mutations

akin to those commonly observed in human HGSCs. The transformed cells retain the capacity to differentiate along multiple Müllerian sublineages, both epithelial and mesenchymal. Notably, in contrast to the (*Amhr2*) *Dicer-Pten* double-knockout mice described by Kim *et al.*, in which tumours initially arise in the oviductal stroma [17], the first recognizable lesions in our models are in the FTE. We have previously shown that, like PAX8, OVGPI is expressed primarily in secretory, rather than ciliated, cells in the mouse FTE [22]. Not surprisingly, transformation of OVGPI-expressing cells results in tumours that express PAX8, a marker of secretory cells, but not tubulin, which is expressed by ciliated cells. The mucinous differentiation of oviductal epithelium noted in TAM-treated *BPP* mice was not seen in *BPR*, *BPN* or *BPRN* mice, suggesting a role for *Pten* inactivation in driving this metaplastic change. We have also observed squamous differentiation in occasional tumours arising in the context of *Brcal*, *Trp53* and *Pten* inactivation (not shown). Mucinous and/or squamous differentiation is commonly seen in human endometrioid carcinomas, which have a high frequency of *PTEN* mutations [27]. We also

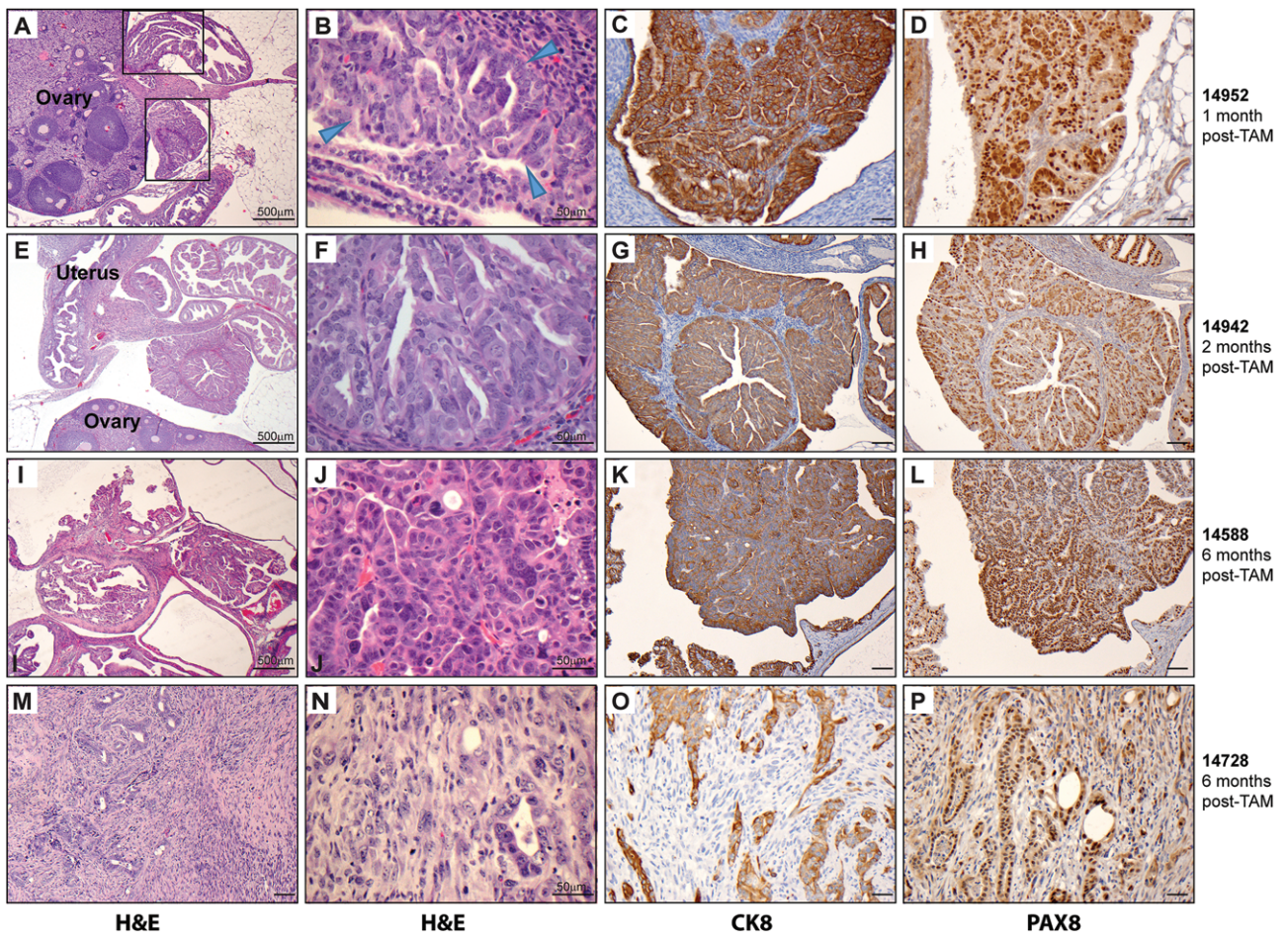


Figure 5. Representative HGSCs and MMTT identified in *BPP* mice at various times after TAM injection. Photomicrographs of H&E-stained and immunostained sections from oviductal STIC and early HGSC identified at 1 month (A–D), early HGSC at 2 months (E–H) and HGSC (I–L) and MMTT with metastasis to ovary (M–P) at 6 months post-TAM injection are shown. The oviduct in (A) shows both STIC (upper boxed area) and early HGSC (lower boxed area). (B), (F), (J) and (N) show higher magnification of the lesions shown in (A), (E), (I) and (M). In (B), the STIC is marked by blue arrowheads. Oviductal tumours arising in *BPP* mice uniformly express CK8 (C, G, K, O) and PAX8 (D, H, L, P).

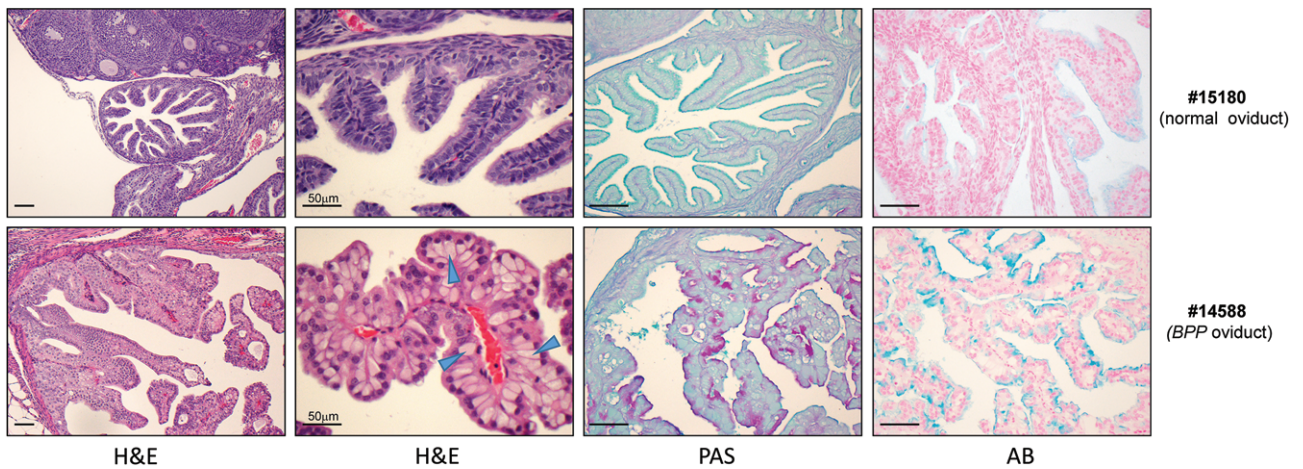


Figure 6. Oviductal epithelium in *BPP* mice shows mucinous metaplasia not seen in *BPR*, *BPN* or *BPRN* mice. The upper panels show normal mouse oviduct stained with H&E (low and high magnification), periodic acid–Schiff (PAS) and Alcian Blue (AB). The lower panels show comparably stained sections of oviduct from a TAM-treated *BPP* mouse. Blue arrowheads point to accumulation of cytoplasmic mucin in the oviductal epithelium of the *BPP* mouse, which is not seen in normal oviduct. The accumulated mucin is positive for both PAS (neutral mucin) and AB (acidic mucin). Note the paucity of PAS-positive or AB-positive mucin in normal oviductal epithelium.

note some differences between the oviductal lesions in our *BPP* mice and those based on transformation of PAX8-positive, rather than OVGP1-positive, cells [18]. Although both models develop STICs and HGSCs that express PAX8, Perets *et al.* [18] did not observe carcinosarcomas or note the diffuse epithelial changes in the oviductal epithelium seen in our *BPP* mice. These differences suggest, but do not prove, that the cells undergoing transformation in the two model systems are not identical. It is also possible that the tumour phenotypes in these two models are influenced by genetic background.

In summary, our GEMMs recapitulate many of the features seen in human HGSCs. The mouse tumours are based on genetic alterations commonly observed in their human tumour counterparts, and arise in the FTE with a predilection for the oviductal equivalent of the human tubal fimbrial epithelium. The histological features and biological behaviour are also similar to those of human HGSC. The models may prove to be particularly useful for studying the early phases of HGSC pathogenesis and the effects of various factors associated with HGSC risk. For example, although women who have had multiple pregnancies or used oral contraceptives are well documented to have a reduced risk of HGSC [28], the mechanisms by which this occurs remain unclear. Our GEMMs could be used to systematically test the effects of these factors on tumour initiation and progression.

Acknowledgements

The research reported in this paper was supported by the National Cancer Institute of the National Institutes of Health under award numbers P30CA046592 (ERF and KRC) and R01CA188516 (KRC, YZ, RW, RK).

Author contributions statement

The authors contributed in the following ways: YZ, RW, RK, ERF, KRC: conceived experiments and analysed data; RW, YZ, MSS, SS, MG: conceived and carried out experiments. All authors were involved in writing the paper, and gave final approval to the submitted version.

References

- Bowtell DD, Bohm S, Ahmed AA, *et al.* Rethinking ovarian cancer II: reducing mortality from high-grade serous ovarian cancer. *Nat Rev Cancer* 2015; **15**: 668–679.
- Piek JM, van Diest PJ, Zweemer RP, *et al.* Dysplastic changes in prophylactically removed Fallopian tubes of women predisposed to developing ovarian cancer. *J Pathol* 2001; **195**: 451–456.
- Kindelberger DW, Lee Y, Miron A, *et al.* Intraepithelial carcinoma of the fimbria and pelvic serous carcinoma: evidence for a causal relationship. *Am J Surg Pathol* 2007; **31**: 161–169.
- Kuhn E, Kurman RJ, Vang R, *et al.* TP53 mutations in serous tubal intraepithelial carcinoma and concurrent pelvic high-grade serous carcinoma—evidence supporting the clonal relationship of the two lesions. *J Pathol* 2012; **226**: 421–426.
- McDaniel AS, Stall JN, Hovelson DH, *et al.* Next-generation sequencing of tubal intraepithelial carcinomas. *JAMA Oncol* 2015; **1**: 1128–1132.
- Eckert MA, Pan S, Hernandez KM, *et al.* Genomics of ovarian cancer progression reveals diverse metastatic trajectories including intraepithelial metastasis to the fallopian tube. *Cancer Discov* 2016; **6**: 1342–1351.
- Cancer Genome Atlas Research Network. Integrated genomic analyses of ovarian carcinoma. *Nature* 2011; **474**: 609–615.
- Patch AM, Christie EL, Etemadmoghadam D, *et al.* Whole-genome characterization of chemoresistant ovarian cancer. *Nature* 2015; **521**: 489–494.
- Kurman RJ, Carcangiu ML, Herrington CS, Young RH (eds). *World Health Organization Classification of Tumours of Female Reproductive Organs* (4th edn). International Agency for Research on Cancer: Lyon, 2014.
- Brustmann H. Ovarian carcinosarcoma associated with bilateral tubal intraepithelial carcinoma: a case report. *Int J Gynecol Pathol* 2013; **32**: 384–389.
- Ardighieri L, Mori L, Conzadori S, *et al.* Identical TP53 mutations in pelvic carcinosarcomas and associated serous tubal intraepithelial carcinomas provide evidence of their clonal relationship. *Virchows Arch* 2016; **469**: 61–69.
- Howell VM. Genetically engineered mouse models for epithelial ovarian cancer: are we there yet? *Semin Cell Dev Biol* 2014; **27**: 106–117.
- Szabova L, Yin C, Bupp S, *et al.* Perturbation of Rb, p53, and Brca1 or Brca2 cooperate in inducing metastatic serous epithelial ovarian cancer. *Cancer Res* 2012; **72**: 4141–4153.
- Connolly DC, Bao R, Nikitin AY, *et al.* Female mice chimeric for expression of the simian virus 40 TAG under control of the MISIR promoter develop epithelial ovarian cancer. *Cancer Res* 2003; **63**: 1389–1397.
- Flesken-Nikitin A, Choi KC, Eng JP, *et al.* Induction of carcinogenesis by concurrent inactivation of p53 and Rb1 in the mouse ovarian surface epithelium. *Cancer Res* 2003; **63**: 3459–3463.
- Flesken-Nikitin A, Hwang CI, Cheng CY, *et al.* Ovarian surface epithelium at the junction area contains a cancer-prone stem cell niche. *Nature* 2013; **495**: 241–245.
- Kim J, Coffey DM, Creighton CJ, *et al.* High-grade serous ovarian cancer arises from fallopian tube in a mouse model. *Proc Natl Acad Sci U S A* 2012; **109**: 3921–3926.
- Perets R, Wyant GA, Muto KW, *et al.* Transformation of the fallopian tube secretory epithelium leads to high-grade serous ovarian cancer in brca;tp53;pten models. *Cancer Cell* 2013; **24**: 751–765.
- Arango NA, Kobayashi A, Wang Y, *et al.* A mesenchymal perspective of Mullerian duct differentiation and regression in Amhr2-lacZ mice. *Mol Reprod Dev* 2008; **75**: 1154–1162.
- Ordóñez NG. Value of PAX 8 immunostaining in tumor diagnosis: a review and update. *Adv Anat Pathol* 2012; **19**: 140–151.
- Miyoshi I, Takahashi K, Kon Y, *et al.* Mouse transgenic for murine oviduct-specific glycoprotein promoter-driven simian virus 40 large T-antigen: tumor formation and its hormonal regulation. *Mol Reprod Dev* 2002; **63**: 168–176.
- Wu R, Zhai Y, Kuick R, *et al.* Impact of oviductal versus ovarian epithelial cell of origin on ovarian endometrioid carcinoma phenotype in the mouse. *J Pathol* 2016; **240**: 341–351.
- Olive KP, Tuveson DA, Ruhe ZC, *et al.* Mutant p53 gain of function in two mouse models of Li–Fraumeni syndrome. *Cell* 2004; **119**: 847–860.
- Anisimov VN, Ukraintseva SV, Yashin AI. Cancer in rodents: does it tell us about cancer in humans? *Nat Rev Cancer* 2005; **5**: 807–819.

25. Son WC, Gopinath C. Early occurrence of spontaneous tumors in CD-1 mice and Sprague–Dawley rats. *Toxicol Pathol* 2004; **32**: 371–374.
26. Reuber MD, Vlahakis G, Heston WE. Spontaneous hyperplastic and neoplastic lesions of the uterus in mice. *J Gerontol* 1981; **36**: 663–673.
27. Obata K, Morland SJ, Watson RH, *et al.* Frequent PTEN/MMAC mutations in endometrioid but not serous or mucinous epithelial ovarian tumors. *Cancer Res* 1998; **58**: 2095–2097.
28. Sopik V, Iqbal J, Rosen B, *et al.* Why have ovarian cancer mortality rates declined? Part I. Incidence. *Gynecol Oncol* 2015; **138**: 741–749.

SUPPLEMENTARY MATERIAL ONLINE

Supplementary figure legends

Figure S1. Metastatic HGSC to ovary in *BPRN* mouse (#13576)

Figure S2. Representative photomicrographs of tubulin and PAX8 expression in STIC and HGSC

Figure S3. Cre-mediated gene recombination evaluated by PCR in genomic DNA isolated from representative matched mouse tails and oviductal tumours

Figure S4. Recombination status of engineered *Rb1*, *Brca1*, *Trp53* and *Nfl* alleles in DNA isolated from representative matched tails and non-oviductal tumours

Table S1. PCR primers for genotyping

Table S2. Summary of oviductal tumour phenotype and non-oviductal tumours in TAM-treated *BPRN*, *BPR* and *BPN* mice

Table S3. Summary of oviductal tumour phenotype in TAM-treated *BPP* mice

75 Years ago in the *Journal of Pathology*...

On the nature of mouse lung adenomata, with special reference to the effects of atmospheric dust on the incidence of these tumours

Stuart McDonald Jr and D. L. Woodhouse

The significance of the potentials developed at noble metal electrodes immersed in cultures of *Bact. coli* in a synthetic medium

K. I. Johnstone

Natural relative hypoplasia of organs and the process of ageing

Dr V. Korenchevsky

To view these articles, and more, please visit:

www.thejournalofpathology.com

Click 'ALL ISSUES (1892 - 2017)', to read articles going right back to Volume 1, Issue 1.

The Journal of Pathology
Understanding Disease

